

THE EFFECT OF ION-BEAM INDUCED STRAIN ON THE NUCLEATION DENSITY OF CHEMICAL VAPOUR DEPOSITED DIAMOND.

P.S. Weiser, S. Praver, K.W. Nugent, A.A. Bettioli, L.I. Kostidis, S.P. Dooley and D.N. Jamieson.
Micro Analytical Research Centre, School of Physics, University of Melbourne, Parkville,
Victoria 3052, Australia.

The effect of ion implantation on the nucleation of CVD diamond on silicon and diamond substrates has been investigated. The strategy employed is to create laterally confined regions of strain in the substrates by focused MeV implantation of light ions. Raman Microscopy has been employed to obtain spatially resolved maps of the strain in these implanted regions. On diamond substrates a homo-epitaxial CVD diamond film was grown on top of both the implanted and unimplanted regions of the substrate. Raman analysis of the film grown on top of the implanted region revealed it to be under slightly tensile strain as compared to that grown on the unimplanted diamond substrate. The film deposited on the implanted portion of the diamond showed a lower fluorescence background; indicating a lower concentration of incorporated defects. These results suggest that the strain and defects in the diamond substrate material have an important influence on the quality of the homo-epitaxially grown diamond films.

Introduction

The nucleation of CVD diamond is a complicated process, governed by many interrelated parameters. In the present work we attempt to elucidate the effect of strain on the nucleation and growth of CVD diamond. We employ laterally confined high dose (MeV) Helium and Hydrogen ion implantation to produce surface swelling of the substrate. The swollen regions are highly stressed but, despite the high level of strain, the surface of the substrate remains relatively undamaged. This is because the nuclear stopping power of these light ions at the substrate surface is small. The strain is enhanced by the lateral confinement of the implanted region to squares of 60×60 or $100 \times 100 \mu\text{m}^2$. In this way, it is possible to produce relatively undamaged, but very substantially strained, surface layers. Silicon substrates were employed in order to study the effect of strain on the hetero-epitaxial growth of CVD diamond film, whilst single crystal diamond substrates were used to study the effect of strain on homo-epitaxial growth. After ion implantation, both substrates were analysed by micro-Raman spectroscopy in order to map the surface strain. The substrates were then inserted into a CVD reactor and diamond was grown upon them. Since the strained regions

were laterally confined, it was then possible to monitor the effect of strain on diamond nucleation.

Experiment

The substrates of (100) Silicon ($2-5 \Omega/\text{cm}^2$) were ultrasonically cleaned in organic solvents prior to being mounted on an Aluminium target holder. The substrates were then inserted into the Micro-Analytical Research Centre's (MARC) Nuclear Microprobe and evacuated to a base pressure better than 5×10^{-6} Torr. The Si samples were then implanted with 2 MeV He and 2 MeV H^+ ions over an area of $60 \times 60 \mu\text{m}^2$ over the dose range 3×10^{16} to 2×10^{18} ions/ cm^2 in both channelled and random orientations. (The ion range and straggling, as predicted by TRIM90 [1], for randomly aligned 2 MeV He ions into Si are $7.07 \mu\text{m}$ and $0.18 \mu\text{m}$ respectively.) The diamond substrates used were $3 \times 3 \text{mm}^2$ (100) natural diamonds from Argyle diamond mines. The diamond substrates were also implanted with 2 MeV He and H^+ ions in the random orientation over an area of $100 \times 100 \mu\text{m}^2$ over a dose range of 1.0×10^{15} to 1.0×10^{18} ions/ cm^2 . (The ion range and straggling, as predicted by TRIM90 [1], for randomly aligned 2 MeV He ions into diamond are $5.36 \mu\text{m}$ and $0.08 \mu\text{m}$ respectively.) Further

information regarding the implantation technique can be found in ref. [2]. The implanted squares were analysed using a surface profilometer and micro-Raman spectroscopy.

The Raman measurements were taken using a Dilor XY confocal micro-Raman spectrometer employing the 514 nm line from an Ar ion laser with a $\times 100$ objective and a confocal aperture of 50 μm . The optical arrangement is such that, even though diamond is transparent to the 514 nm light used in the Raman measurement, the sampling volume is restricted to a cylinder of diameter 1 μm and depth 2 μm . For silicon substrates, the analysis depth is further restricted by the depth of penetration of the laser light into the silicon, which is about 0.5 μm . Hence, for silicon, the Raman measurement samples only the swollen cap above the end of range damage, whilst for the diamond a depth scan is possible by varying the position of the focus of the laser. Strain within a material has been shown to produce shifts in the position of the peaks in the Raman spectra. The Raman shift to higher energy is indicative of compressive strain, while a shift to lower energy is indicative of tensile strain. [3].

After Raman analysis the samples were inserted into the CVD deposition system. The microwave assisted CVD deposition conditions for the silicon samples were as follows: pressure 20 Torr; total flow 100 sccm; 1% CH_4 ; deposition temperature 1050°C and deposition time 12 hours. The Hot filament assisted CVD deposition conditions for the diamond samples were as follows: pressure 30 Torr; total flow 100 sccm; 1% CH_4 ; deposition temperature 1000°C and deposition time 4 hours. The choice of either microwave or hot-filament CVD deposition system was determined by the physical size and shape of the substrate. The conditions used in both systems were those that are known to produce optimum film growth for that system. After CVD diamond deposition the samples were re-analysed using surface profilometry and micro-Raman Spectroscopy.

Results and Discussion

Silicon Substrates:

Prior to CVD deposition a Raman linescan was performed on the 8.56×10^{17} ions/cm² channelled He implant. The position of the Si Raman line, as a function of distance across the implant, is shown in figure 1. The position of the 520 cm⁻¹ peak shifted ~ 2.3 cm⁻¹ to lower energy across most of the implanted square, however the FWHM shows only a $\sim 25\%$ increase, indicating that little surface damage has occurred as a result of the ion implantation (figure 2). The edges of the implanted square show a shift of the Raman line to higher energy by on average 1.5 cm⁻¹. These shifts show that, while the Si surface at the top of the implanted square is under tensile strain, the edges of the implanted region are under compressive strain. Also shown in figure 1 is the surface height profile of the implant. This shows that the surface of the implant is raised 370 nm.

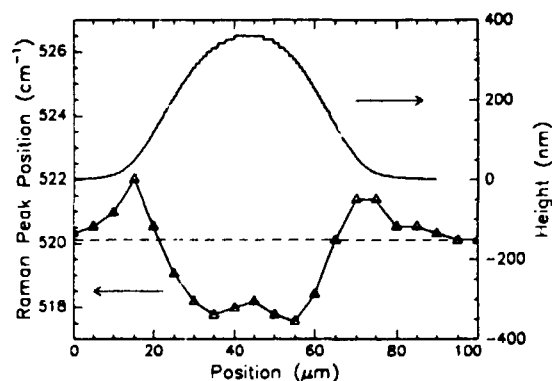


Figure 1. Raman peak position as a function of distance across a 8.56×10^{17} ions/cm² channelled He implant. The size of the implant was $60 \times 60 \mu\text{m}^2$. The position for unimplanted Si is 520.1 cm⁻¹ this is marked by a dotted line. Also shown is the surface height profile across the implant.

After CVD deposition it became obvious that for doses exceeding 1.6×10^{17} ions/cm² of channelled 2 MeV He ions, the entire implanted region has been removed. For example, figure 2 shows the Raman spectra and the inset, the surface height profile for the 1.98×10^{18} ions/cm² random implant before

and after exposure to the CVD plasma. It is obvious that, post CVD, a deep crater has been formed. The crater for the random implants is, on average, $7.2 \pm 0.2 \mu\text{m}$ with the depth of the crater from the channelled implants being, on average, $8.2 \pm 0.2 \mu\text{m}$. The depth of the crater for the random implants is equal to the ion range as predicted by TRIM90 [1]. The regions implanted to doses around 1.6×10^{17} ions/cm² show no detectable shift in the position of the Si Raman peak and little swelling ($0.04 \mu\text{m}$) prior to CVD diamond deposition. After CVD diamond deposition these implants show the capped Si layer to have swollen ($3.10 \mu\text{m}$) and split (at least on one of the four sides), probably relieving pressure in the process. Loss of the implanted region in the higher doses was also found to occur following annealing in a furnace at 1000°C . Hence, we conclude that the most likely origin of the loss is the expansion of the implanted He or H bubbles at the end of range. These results suggest that it may be necessary to implant with non-gaseous implant species in order to use this method to investigate the effect of the strain distribution on the hetero-epitaxial nucleation of CVD diamond.

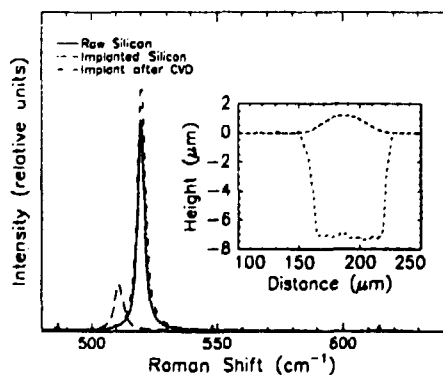


Figure 2. Raman spectra of the Si Raman line of virgin and 1.98×10^{18} ions/cm² He implanted Si before and after CVD diamond deposition for 12 hours. The inset shows the surface height profile of a 1.98×10^{18} ions/cm² implant before and after 12 hours of CVD diamond deposition conditions.

Diamond Substrates:

Figure 3 shows the shift in the Raman diamond line position in steps of $5 \mu\text{m}$ across

a $100 \times 100 \mu\text{m}^2$ 2 MeV random He implant of dose 5.0×10^{17} ions/cm². The Raman diamond line position from the surface of the implant is shifted to lower energy by, on average, 5.4 cm^{-1} (FWHM, 12 cm^{-1}) from its unstrained value of 1331.32 cm^{-1} (FWHM, 3.2 cm^{-1}). As distinct from the Si case, the diamond line is broadened. This indicates that the strain in the cap is caused by defects in the cap, rather than by the end of range damage [4]. Recently, K.W. Nugent et al [5] have identified two new Raman peaks at 1497 and 1630 cm^{-1} associated with damage centres in diamond. Figure 3 plots the ratio of the 1497 cm^{-1} defect peak to that of the 1332 cm^{-1} diamond line across the surface of the implant. The presence of the 1497 cm^{-1} peak confirms that the strain is induced by defects in the cap layer itself. Surface profilometry measurements show that the 5.0×10^{17} ions/cm² implant has raised the diamond surface by $0.13 \mu\text{m}$.

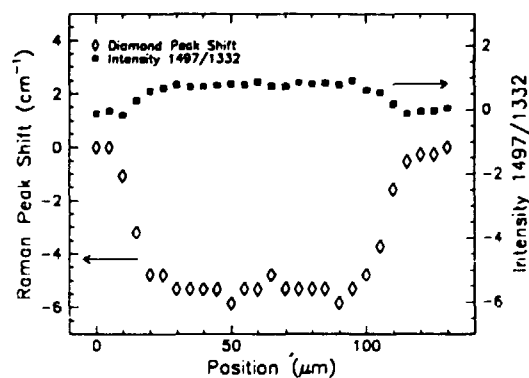


Figure 3. The Raman diamond peak position as a function of position across a $100 \times 100 \mu\text{m}^2$ region which has been implanted with 2 MeV He ions to a dose of 5.0×10^{17} ions/cm². Also shown is the ratio of the intensity of the Raman peak at 1497 cm^{-1} (due to damage) to the that of the Raman diamond peak as a function of distance across the implanted region.

After CVD, optical microscopy showed that a film has grown over the entire surface of the diamond substrate. Surface profilometry of the implant post CVD reveals a step height of, on average, $0.14 \mu\text{m}$. This is the same as the step height of the implant prior to CVD. Therefore, the rate of diamond film

growth on the implanted and unimplanted diamond substrate is the same.

Before CVD, the implanted region is clearly visible as a black square in the diamond. After CVD much of the strong absorption appears to have disappeared, indicating that most of the defects associated with the implantation have probably been annealed.

The deposited film was established as being homo-epitaxial, with respect to the substrate, by comparing polarised Raman azimuthal scans of the surface of the deposited diamond film and of the underlying diamond substrate at a depth greater than 8 μm below the surface [see ref. 6 for details of this technique].

After CVD, the Raman spectra were once again performed across the surface of the 5.0×10^{17} ions/cm² implant. The shift in the diamond line across the implant is plotted in figure 4 (the shift across the implant prior to the CVD is also shown). The diamond line of the implant is still shifted to lower energy but only on average by 1.1 cm⁻¹. There is no evidence of the 1497 and 1630 cm⁻¹ damage peaks. In addition, the FWHM of the diamond line is 3.7 cm⁻¹, which is similar to the FWHM of the unimplanted diamond substrate of 3.2 cm⁻¹. The absence of the damage peaks and the shift in the diamond line back towards its unstrained value could be due to either (i) the growth of an epitaxial film or alternatively (ii) to the annealing of the ion-induced damage which has been observed at these temperatures [5]. For this reason a depth scan of the Raman spectra in the implanted region was performed. Figure 5 shows the ratio of the intensity of the 1497 cm⁻¹ damage peak to the diamond line on the 5.0×10^{17} ions/cm² implant as a function of depth from the surface. The 1497 cm⁻¹ peak is absent for the first 5 μm of the depth profile, but then its value rises and reaches a steady value about 10 μm below the surface. There is no change in the diamond line position or FWHM throughout the depth profile. These results are consistent with an incompletely annealed implanted layer lying underneath a 5 μm thick homo-epitaxial diamond film. Whatever the

origin of the 1497 cm⁻¹ defect, it does not propagate into the grown CVD film.

Surprisingly, the Raman spectra of the film grown on the unimplanted diamond shows a large fluorescent background, which is not observed from the film grown on the implanted region. The inset to figure 5 is a depth profile performed on the film grown on the unimplanted diamond, showing the ratio of the fluorescent background intensity to that of the diamond. The large fluorescent background is present for the first 5 μm , consistent with the thickness of the diamond film grown on the diamond substrate. Since fluorescence is indicative of the presence of defects, the lower fluorescent yield for the diamond deposited on top of the implanted region may indicate that it contains a lower defect density than that grown on top of the unimplanted diamond. Clearly this unexpected, but potentially important result, will require further verification. At present, we speculate that there may be a connection between the lower fluorescent background and the tensile strain in the film.

Conclusion

In order to investigate the effect of strain on the nucleation density of CVD deposited diamond we have employed high dose Helium and Hydrogen ion implantation into both silicon and diamond substrates, to produce surface swelling of the substrate. Raman spectroscopy revealed that the surfaces of the implanted regions are under tensile strain (up to 4.5 GPa). Despite the high level of strain, the implanted surface of the silicon remains relatively undamaged, with the FWHM of the Raman peak virtually unchanged from that of the unimplanted silicon. However, for ion doses above 1.6×10^{17} ions/cm², the large concentration of implanted H or He at the end of range results in the delamination of the entire implanted region upon CVD diamond deposition or furnace annealing at 1000°C. For diamond, delamination of the implanted region does not occur even for very high ion doses. The growth rate of homoepitaxial diamond is the same on the implanted and unimplanted

regions of the diamond substrate. However, the CVD film grown on the implanted region shows slight residual tensile strain, but a reduced fluorescent yield as compared with the film grown on the unimplanted diamond substrate.

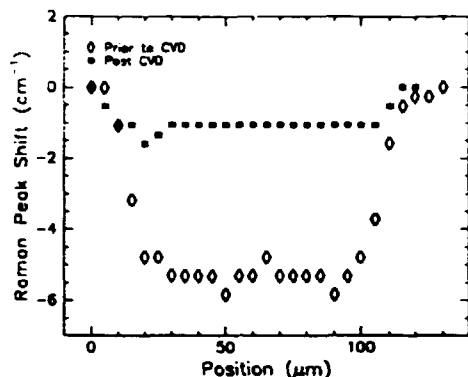


Figure 4. The Raman diamond peak position as a function of position across a $100 \times 100 \mu\text{m}^2$ region implanted with 2 MeV He ions to a dose of 5.0×10^{17} ions/cm² after 4 hours of CVD diamond deposition. Overlaid is the Raman diamond peak position as a function of position across the implant prior to CVD.

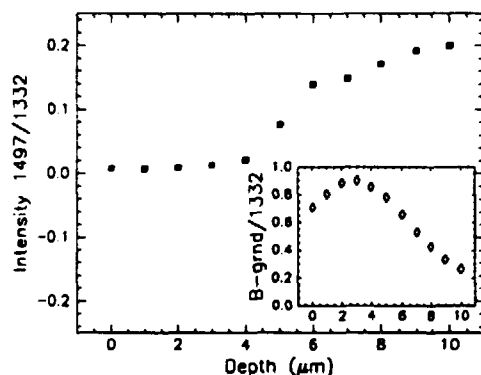


Figure 5. The ratio of the intensity of the 1497 cm^{-1} damage peak to that of the diamond line (on the 5.0×10^{17} ions/cm² implant) as a function of depth after 4 hours of CVD diamond deposition. The inset shows the ratio of the fluorescent background to the diamond peak intensity as a function of depth into the diamond film grown on the unimplanted diamond substrate

References

- [1] TRIM90 - J.F. Ziegler and J.P. Biersack, *The Stopping and Ranges of Ions in Solids*, (Pergamon, New York, 1988).
- [2] S.P. Dooley and D.N. Jamieson, *Nuclear Instruments and Methods in Physics Research B66*, 369-373, (1992).
- [3] D.S. Knight and W.B. White, *J. Mater. Res.*, 4, 385, 1989.
- [4] D.N. Jamieson, S. Prawer, K.W. Nugent and S.P. Dooley, Presented at IBMM'95.
- [5] K.W. Nugent, S.P. Dooley, S. Prawer and D.N. Jamieson, In Preparation.
- [6] P. John, D.K. Milne, P.G. Roberts, M.G. Jubber, M. Liehr and J.I.B. Wilson, *J. Mater. Res.*, 9(12), 3083, 1994